

***N*-Dimensional Chaotic Attractors with Crystallographic Symmetry**

(preprint)

Jeffrey P. Dumont,^a Flynn J. Heiss,^b Kevin C. Jones,^c
Clifford A. Reiter,^{d,*} and Lisa M. Vislocky^e

^a Lafayette College, Box 7756, Easton PA 18042, U.S.A.

^b 57 Main Street, Geneseo NY 14454, U.S.A.

^c 3329 25th Avenue, Moline IL 61265, U.S.A.

^d Department of Mathematics, Lafayette College, Easton PA 18042, U.S.A.

^e 222 Slater Boulevard, Staten Island, NY 10305, U.S.A.

Abstract --- Chaotic attractors with planar symmetries have been the focus of much recent study. We establish a general method to create attractors with crystallographic symmetry in \mathcal{R}^n . Using this technique we provide a uniform approach to creating chaotic attractors in \mathcal{R}^2 and generate provocative illustrations in \mathcal{R}^3 with crystallographic symmetry.

1. INTRODUCTION

Symmetry is associated with structure and order. In [1], Weyl says symmetry “is one idea by which man through the ages has tried to comprehend and create order, beauty and perfection”. On the other hand, chaos is associated with disorder and randomness. Gleick [2] has popularized the butterfly effect which illustrates the sensitivity to initial conditions inherent in chaotic behavior and observed in the weather model of Lorenz [3]. Remarkably, symmetry is compatible with chaos. One sees turbulence with symmetry in Couette-Taylor flows [4] and structure with randomness in snowflakes [5]. A wide range of patterns with underlying chaos is discussed in [6].

Much recent work has been done creating chaotic attractors with planar and point group symmetry. Various techniques for creating such attractors are explored in [7-15]. A simple and elegant group summation technique was developed in [12] to create chaotic attractors with cyclic and dihedral symmetry. When such point group symmetry is compatible with a lattice, similar methods are used to create chaotic attractors with that symmetry [10]. However, not all planar crystallographic groups can be generated using the constructions from that paper. This paper develops general techniques that allow chaotic attractors with any crystallographic symmetry to be created. In contrast to the various innovations used to handle different kinds of planar symmetry groups in [8], this paper provides a general unified method (described in Theorem 6 and Porism 7) for creating chaotic attractors with the symmetry of all of the planar crystallographic groups. Moreover, this technique works well for creating chaotic attractors with three-dimensional crystallographic space group symmetry and could be used in any dimension.

* Author for correspondence: C. A. Reiter. E-mail: reiterc@lafayette.edu

The diversity of the three-dimensional space groups is remarkable. They are enumerated in the *International Tables for Crystallography* [16] and expositied upon in [17]. It is intriguing that, because of the importance of these groups in studying crystals, the 230 space groups were determined before the 17 planar groups were enumerated [18]. In addition to illustrating our techniques in the plane, our investigation explores the 24 examples of space groups given in the teaching edition of the International Tables [19]. This paper highlights five of these 24 space group examples. Animations for these 24 space groups may be found at the web address <http://www.lafayette.edu/~reiterc/cacs>.

2. Functions with Crystallographic Symmetry

Symmetries of an object in \mathfrak{R}^n are isometries, that is, distance preserving maps. A group of symmetries is crystallographic if its subgroup of translation vectors is a lattice in \mathfrak{R}^n . In this section we develop the mathematical theory required to allow us to construct functions with any desired crystallographic symmetry. The following definition gives the property required for a function to have a desired symmetry.

Definition. A function $f : \mathfrak{R}^n \rightarrow \mathfrak{R}^n$ is *equivariant* with respect to a symmetry σ if $f(\sigma(\vec{x})) = \sigma(f(\vec{x}))$ for all $\vec{x} \in \mathfrak{R}^n$.

If a function is equivariant with respect to the symmetries in a group, the attractor associated with the iteration of that function may degenerate and have more symmetry. On the other hand, the attractor may only form one component from a collection of conjugate attractors and hence have less symmetry. However, nontrivial attractors created by such equivariant functions typically demonstrate the desired symmetry. We are content to visually verify that our attractors have the specified symmetry. However, computational techniques for determining the symmetry of attractors have been studied [20].

Our theory develops in stages. The first three propositions generalize results in [10]. The first proposition gives a construction providing equivariance with respect to the translational symmetries of a lattice. We next consider point group symmetry and then combine that symmetry with translational symmetry where the point group is compatible with the lattice. Our main results (Theorem 6 and Porism 7) deal with the more general situation where the crystallographic group does not preserve the lattice.

We begin by constructing functions equivariant with respect to the translational symmetries of a lattice L which is generated by n linearly independent n -dimensional vectors. With L given, we can determine a dual lattice L^* such that if $\vec{u} \in L$ and $\vec{v} \in L^*$, then $\vec{u} \cdot \vec{v} \in \mathbb{Z}$. If instead we choose \vec{v} from $2\pi L^*$, then $\vec{u} \cdot \vec{v} \in 2\pi\mathbb{Z}$. In this case, $\cos(\vec{v} \cdot (\vec{x} + \vec{u})) = \cos(\vec{v} \cdot \vec{x})$ since $\vec{v} \cdot \vec{u}$ is an integer multiple of 2π . The corresponding statement is also true for the sine function.

Proposition 1. Let L be a lattice in \mathfrak{R}^n , L^* be the dual lattice for L and V be any finite subset of $2\pi L^*$. Also for all $\vec{v} \in V$ let there be associated constant parameter vectors $\vec{\alpha}_{\vec{v}}, \vec{\beta}_{\vec{v}} \in \mathfrak{R}^n$. Then the function f_v defined by

$$f_V(\vec{x}) = \sum_{\vec{v} \in V} (\vec{\alpha}_{\vec{v}} \cos(\vec{v} \cdot \vec{x}) + \vec{\beta}_{\vec{v}} \sin(\vec{v} \cdot \vec{x}))$$

is equivariant with respect to the translational symmetries of L .

Proof. We need to show that for any $\vec{u} \in L$ we have $f_V(\vec{x}) + \vec{u} \equiv f_V(\vec{x} + \vec{u}) \pmod{L}$.

Clearly $f_V(\vec{x}) + \vec{u} \equiv f_V(\vec{x}) \pmod{L}$, while

$$f_V(\vec{x} + \vec{u}) = \sum_{\vec{v} \in V} (\vec{\alpha}_{\vec{v}} \cos(\vec{v} \cdot (\vec{x} + \vec{u})) + \vec{\beta}_{\vec{v}} \sin(\vec{v} \cdot (\vec{x} + \vec{u}))) = \sum_{\vec{v} \in V} (\vec{\alpha}_{\vec{v}} \cos(\vec{v} \cdot \vec{x}) + \vec{\beta}_{\vec{v}} \sin(\vec{v} \cdot \vec{x})) = f_V(\vec{x})$$

by the remarks preceding this proposition. Hence $f_V(\vec{x}) + \vec{u} \equiv f(\vec{x} + \vec{u}) \pmod{L}$, as required. \square

Figure 1 gives an illustration of a chaotic attractor in \mathfrak{R}^2 created by a function of the form defined in Proposition 1. This figure will be further explained in Section 4. For now, notice that the only symmetry in the illustration is the symmetry of horizontal and vertical translations.

Proposition 2. Let $f: \mathfrak{R}^n \rightarrow \mathfrak{R}^n$ be an arbitrary function and let G be a finite group realized by n by n matrices acting on \mathfrak{R}^n by multiplication on the right. Then

$$h_{f,G}(\vec{x}) = \sum_{\sigma \in G} \sigma^{-1}(f(\sigma(\vec{x})))$$

is equivariant with respect to the elements of G .

Proof. Let $\gamma \in G$. We need to show that $h_{f,G}(\gamma(\vec{x})) = \gamma(h_{f,G}(\vec{x}))$. We see that

$$h_{f,G}(\gamma(\vec{x})) = \sum_{\sigma \in G} \sigma^{-1}(f(\sigma(\gamma(\vec{x})))) = \sum_{\sigma \in G} \gamma \sigma^{-1} \sigma^{-1}(f(\sigma \gamma(\vec{x}))) = \sum_{\sigma \in G} \gamma (\sigma \gamma)^{-1}(f(\sigma \gamma(\vec{x})))$$

$$= \gamma \sum_{\sigma \in G} (\sigma \gamma)^{-1}(f(\sigma \gamma(\vec{x}))), \text{ since matrix multiplication is distributive. Also, } \sigma \gamma \text{ runs}$$

through all of the elements of G as σ does, so the above is equal to

$$\gamma \sum_{\sigma \in G} \sigma^{-1}(f(\sigma(\vec{x}))) = \gamma(h_{f,G}(\vec{x})) \text{ as required. } \square$$

Figure 2 gives an illustration of a chaotic attractor in \mathfrak{R}^2 created by a function of the form defined in Proposition 2 with $G = D_7$. This dihedral group contains 7-fold rotational symmetry, as well as 7 mirrors through the center of rotation. Notice that the illustration does not contain translational symmetry in either direction, only the rotations and mirrors. This figure will be further explained in Section 4.

Corollary 3 will follow as a special case of Porism 7, but we state it here because it is a natural step of combining translational and rotational symmetry.

Corollary 3. If $f_V(\vec{x})$ is defined as in Proposition 1, and G maps the lattice L back onto itself, then $h_{f_V,G}(\vec{x}) \pmod{L}$ as defined in Proposition 2 is equivariant with respect to both the lattice and the symmetries of $G \pmod{L}$.

Figure 3 is created by a combination of functions as described in Corollary 3. Notice the 3-fold rotational symmetry, the mirrors, as well as the hexagonal translational symmetry.

To deal with the general crystallographic groups, we need to be able to handle symmetries that do not preserve the lattice but which have enough structure so that we can create functions with the desired equivariance property. The following example illustrates such a symmetry.

Example. In space group 19 in the International Tables [11], the second listed symmetry

is written as $\begin{pmatrix} \bar{x} + 1/2 \\ \bar{y} \\ z + 1/2 \end{pmatrix}$. That symmetry is the map $p \begin{pmatrix} x \\ y \\ z \end{pmatrix} = \begin{pmatrix} 1/2 - x \\ -y \\ 1/2 + z \end{pmatrix} \bmod L$, which sends

$\begin{pmatrix} 0 \\ 0 \\ 0 \end{pmatrix}$, a point in the lattice, to $\begin{pmatrix} 1/2 \\ 0 \\ 1/2 \end{pmatrix}$, which is not a point on the integer lattice. Notice

that this symmetry is the composition of the maps $\mu \begin{pmatrix} x \\ y \\ z \end{pmatrix} = \begin{pmatrix} -1 & 0 & 0 \\ 0 & -1 & 0 \\ 0 & 0 & 1 \end{pmatrix} \begin{pmatrix} x \\ y \\ z \end{pmatrix}$ and

$\tau \begin{pmatrix} x \\ y \\ z \end{pmatrix} = \begin{pmatrix} x \\ y \\ z \end{pmatrix} + \begin{pmatrix} 1/2 \\ 0 \\ 1/2 \end{pmatrix}$. That is, $p = \tau\mu$. Indeed, affine transformations are exactly those

maps that can be decomposed into a linear and translational part.

To simplify the implementation of functions with these symmetries, we can represent such symmetries via a single matrix in homogeneous coordinates. For

example, $\begin{pmatrix} x \\ y \\ z \end{pmatrix}$ would become $\begin{pmatrix} x \\ y \\ z \\ 1 \end{pmatrix}$ in homogenous coordinates. We see

$\begin{pmatrix} -1 & 0 & 0 & 1/2 \\ 0 & -1 & 0 & 0 \\ 0 & 0 & 1 & 1/2 \\ 0 & 0 & 0 & 1 \end{pmatrix} \begin{pmatrix} x \\ y \\ z \\ 1 \end{pmatrix} = \begin{pmatrix} 1/2 - x \\ -y \\ 1/2 + z \\ 1 \end{pmatrix}$, which shows that, after switching back to ordinary

coordinates, $\begin{pmatrix} x \\ y \\ z \end{pmatrix}$ is sent to $\begin{pmatrix} 1/2 - x \\ -y \\ 1/2 + z \end{pmatrix}$, as required. Thus, the symmetry p can be

represented by the matrix $\begin{pmatrix} -1 & 0 & 0 & 1/2 \\ 0 & -1 & 0 & 0 \\ 0 & 0 & 1 & 1/2 \\ 0 & 0 & 0 & 1 \end{pmatrix}$ in homogeneous coordinates. This is the

form we use in our implementation.

The following definition captures properties of crystallographic groups mod L , where L is a lattice. These properties hold for the representations given for the two and three dimensional crystallographic groups in [16] and the four dimensional crystallographic groups in [21].

Definition. Given a lattice L in \mathfrak{R}^n , we define a **position group** P on L as a finite group of affine transformations mod L such that for all elements p of P , when we write $p = \tau\mu$ where τ is a translation and μ is a linear transformation, then μ sends all elements of L back to L and $|P|\tau(\vec{0}) \equiv \vec{0} \pmod{L}$ where $|P|$ denotes the order of P .

Remark: In particular, crystallographic groups modulo their lattice can be presented in the form of a position group. Basically, the condition that $|P|\tau(\vec{0}) \equiv \vec{0} \pmod{L}$ guarantees that the denominators appearing in the translational part divide the order of the position group. It is known that any crystallographic group is isomorphic to a group which is generated by affine transformations with the linear part coming from a finite group of unimodular transformations and the corresponding translational components satisfying $|P|\tau(\vec{0}) \equiv \vec{0} \pmod{Z}$. In this situation, we think of the position group as described in terms of coordinates with respect to a basis; hence mod Z corresponds to what we previously denoted mod L . See Speiser's Theorem in [22, p161] or [23]. The presentations of the two and three dimensional crystallographic groups in [16] and the four dimensional crystallographic groups in [21] are expressed in the form of position groups and hence may be used directly in our constructions.

The following two lemmas allow us to begin to make explicit the effects of the translational parts of symmetries of position groups.

Lemma 4. *Let L be a lattice in \mathfrak{R}^n , let P be a position group on L , let $p \in P$ and let $p = \tau\mu$ be the decomposition where τ is a translation and μ is a linear transformation. Then*

- (i) $\tau(\vec{x}) = \vec{x} + \tau(\vec{0})$ for all \vec{x} in \mathfrak{R}^n ,
- (ii) $p(\vec{0}) = \tau(\vec{0})$,
- (iii) if $\vec{w} \in L$, $p(\vec{w}) - p(\vec{0}) \in L$.

Proof. (i) Since τ is a translation, it moves every point the same amount as it moves $\vec{0}$.
(ii) $p(\vec{0}) = \tau(\mu(\vec{0})) = \tau(\vec{0})$ since $\mu(\vec{0}) = \vec{0}$ by the linearity of μ .
(iii) Using (ii), we see $p(\vec{w}) - p(\vec{0}) = \tau\mu(\vec{w}) - \tau(\vec{0}) = \tau(\vec{w}') - \tau(\vec{0})$, where \vec{w}' is an element of L since our definition of a position group requires μ to send elements of L to L . By (i), $p(\vec{w}) - p(\vec{0}) = \vec{w}' + \tau(\vec{0}) - \tau(\vec{0}) = \vec{w}' \in L$. \square

Lemma 5. Let L be a lattice in \mathfrak{R}^n , let P be a position group on L and let $p \in P$. Then

$$p\left(\sum_{i=1}^m (\vec{x}_i)\right) = \left(\sum_{i=1}^m p(\vec{x}_i)\right) - (m-1)p(\vec{0}).$$

Proof. Since p is an element of a position group, we know that $p = \tau\mu$, where τ is a translation and μ is a linear transformation. We see that

$$p\left(\sum_{i=1}^m (\vec{x}_i)\right) = p(\vec{x}_1 + \vec{x}_2 + \cdots + \vec{x}_m) = \tau(\mu\vec{x}_1 + \mu\vec{x}_2 + \cdots + \mu\vec{x}_m) = \mu\vec{x}_1 + \mu\vec{x}_2 + \cdots + \mu\vec{x}_m + \tau(\vec{0})$$

by the linearity of μ and Lemma 4 (i). Also,

$$\begin{aligned} \sum_{i=1}^m p(\vec{x}_i) &= p(\vec{x}_1) + p(\vec{x}_2) + \cdots + p(\vec{x}_m) = \mu\vec{x}_1 + \tau(\vec{0}) + \mu\vec{x}_2 + \tau(\vec{0}) + \cdots + \mu\vec{x}_m + \tau(\vec{0}) \\ &= \mu\vec{x}_1 + \mu\vec{x}_2 + \cdots + \mu\vec{x}_m + m\tau(\vec{0}) \text{ using Lemma 4(i) on each term. Since } p(\vec{0}) = \tau(\vec{0}), \text{ as} \\ &\text{shown in Lemma 4(ii), the desired result follows. } \square \end{aligned}$$

We are now prepared to prove our main theorem which gives a construction that may be used to create functions with the symmetry of any crystallographic group.

Theorem 6. Let P be a position group on L , a lattice in \mathfrak{R}^n , and let f be a periodic function mod L . Then the function $i(\vec{x}) = \vec{x} + \sum_{p \in P} p^{-1}(f(p(\vec{x}))) \text{ mod } L$ is equivariant with respect to the translational symmetries of L and the symmetries of P .

Proof. We first show equivariance with respect to L . Let $\vec{w} \in L$. We want to show that $i(\vec{x}) + \vec{w} = i(\vec{x} + \vec{w}) \text{ mod } L$. Since $\vec{w} \in L$, $i(\vec{x}) + \vec{w} = i(\vec{x}) \text{ mod } L$. We need to show that this is equivalent to $i(\vec{x} + \vec{w}) \text{ mod } L$.

$$i(\vec{x} + \vec{w}) = \vec{x} + \vec{w} + \sum_{p \in P} p^{-1}(f(p(\vec{x} + \vec{w}))) = \vec{x} + \sum_{p \in P} p^{-1}(f(p(\vec{x}) + p(\vec{w}) - p(\vec{0}))) \text{ mod } L, \text{ using}$$

Lemma 5 with $m=2$. By Lemma 4(iii), $p(\vec{w}) - p(\vec{0}) = \vec{w}' \in L$. So the above is equal to $\vec{x} + \sum_{p \in P} p^{-1}(f(p(\vec{x}) + \vec{w}')) = \vec{x} + \sum_{p \in P} p^{-1}(f(p(\vec{x})))$, since f is periodic mod L . This is equal to $i(\vec{x})$, hence we have equivariance with respect to the lattice.

We now need to show equivariance with respect to the elements of P . Let $\sigma \in P$. We need to show that $\sigma^{-1}(i(\sigma(\vec{x}))) = i(\vec{x})$. By the definition of $i(\vec{x})$ and Lemma 5 we see

$$\begin{aligned} (*) \quad \sigma^{-1}(i(\sigma(\vec{x}))) &= \sigma^{-1}\left(\sigma(\vec{x}) + \sum_{p \in P} p^{-1}(f(p(\sigma(\vec{x}))))\right) \\ &= \sigma^{-1}(\sigma(\vec{x})) + \sum_{p \in P} \sigma^{-1}(p^{-1}(f(p(\sigma(\vec{x})))) - |P|\sigma^{-1}(\vec{0})). \end{aligned}$$

One term of $-\sigma^{-1}(\vec{0})$ results from the distribution of σ^{-1} over the plus sign while $-(|P|-1)\sigma^{-1}(\vec{0})$ results from the distribution of σ^{-1} over the sigma summation. Notice

that $|P|\sigma^{-1}(\bar{0}) \equiv \bar{0}$ by the definition of position group. Thus equation (*) simplifies to $\bar{x} + \sum_{p \in P} (p\sigma)^{-1}(f(p\sigma(\bar{x}))) \bmod L$ which is $i(\bar{x})$ since $p\sigma$ runs through P as p does. \square

Notice that $i(\bar{x})$ depends on f and P even though the notation does not indicate that fact.

As mentioned before, if the position group maps all of the elements of the lattice L back to L , the function $h_{f,G}(\bar{x})$ as defined in Proposition 2 is equivariant with respect to that group, even without the addition of the auxiliary term \bar{x} which was used in $i(\bar{x})$. If that auxiliary term \bar{x} was missing, then the rightmost term of equation (*) would be $-(|P|-1)\sigma^{-1}(\bar{0})$. This would be $\bar{0}$ because all of the group elements can be represented with only linear transformations, hence $\sigma^{-1}(\bar{0}) = \bar{0}$. This establishes Corollary 3.

We further note that the auxiliary term may be modified in certain situations. The addition of a coordinate from the auxiliary term \bar{x} in $i(\bar{x})$ is only necessary if there exists some element $p = \tau\mu$ such that τ involves a nonzero translation in that coordinate. This is not always necessary, as there are many position groups that involve translations in less than all coordinates. For these groups, it is only necessary to add the coordinates of \bar{x} for which there is a translation in that coordinate. In the coordinates involving no translations, we will get zero from the zero in $-(|P|-1)\sigma^{-1}(\bar{0})$ in those coordinates while if there is a translation, we will get the zero in that coordinate from the corresponding coordinate in $|P|\sigma^{-1}(\bar{0}) \equiv \bar{0}$.

For example, space group 53 as listed in [16] does not involve any non-lattice translations in the y direction, so the function $i'(\bar{x}) = \begin{pmatrix} x \\ 0 \\ z \end{pmatrix} + \sum_{p \in P} p^{-1}(f(p(\bar{x})))$ is equivariant

to the symmetries of P , where P is space group 53 on the standard orthonormal lattice,

and $\bar{x} = \begin{pmatrix} x \\ y \\ z \end{pmatrix}$. This result is presented in the following Porism, which allows us to use a

function with the least variation from that appearing in Corollary 3. That is, when P preserves L a function of the type in Corollary 3 is used; when P preserves no coordinates, a function of the type in Theorem 6 is used; and when P preserves an intermediate number of coordinates, an intermediate function is used.

Porism 7. Let L be a lattice in \Re^n , P be a position group on that lattice, f be a periodic

function mod L , $\bar{x} = \begin{pmatrix} x_1 \\ x_2 \\ \vdots \\ x_n \end{pmatrix}$, and let $x'_i = x_i$ if the i^{th} coordinate of $p(\bar{0})$ is something

other than 0 for some $p \in P$, otherwise let x'_i be 0. Then the function

$$i'(\vec{x}) = \begin{pmatrix} x'_1 \\ x'_2 \\ \vdots \\ x'_n \end{pmatrix} + \sum_{p \in P} p^{-1}(f(p(\vec{x}))) \text{ is equivariant with respect to the translational symmetries}$$

of the lattice and the symmetries of P .

The proof follows from the proof of Theorem 6 in light of the preceding remarks.

3. Implementation

In order to find functions with the symmetries of a given crystallographic group we need to have an explicit representation of the position group. From the International Tables [16], we obtain the generators for the symmetries of a given planar or space group, as in our example in Section 2. Representing these symmetries as matrices in homogeneous coordinates, we compute the group closure using matrix multiplication with the translational part taken mod 1; we thereby enumerate the elements of the position group. We then use this position group to create our functions defined in Porism 7. We have the freedom to select the finite set $V \subset 2\pi L^*$ and the parameters $\vec{\alpha}_{\vec{v}}, \vec{\beta}_{\vec{v}} \in \mathfrak{R}^n$ for all $\vec{v} \in V$.

For the planar groups we selected the parameters at random from between ± 0.5 while for the space groups we tuned the parameter selection and ended up using ranges between ± 0.002 and ± 0.2 . For the planar groups we used $V = 2\pi\{\langle 1,0 \rangle, \langle 0,1 \rangle, \langle 1,1 \rangle\}$. Note that our attractors are defined in position group coordinates and hence when we

required a hexagonal lattice we post-multiplied by the matrix $\begin{pmatrix} 1 & 0 \\ \cos\left(\frac{2}{3}\pi\right) & \sin\left(\frac{2}{3}\pi\right) \end{pmatrix}$ to

obtain the absolute coordinates used for plotting.

For the space groups, we used two different sets of vectors as the set V in Proposition 1. For most of the three-dimensional symmetry groups we used $V_0 = 2\pi\{\langle 1,0,0 \rangle, \langle 0,1,0 \rangle, \langle 0,0,1 \rangle, \langle 1,1,1 \rangle\}$. In some cases that set was inadequate because the attractors had degenerate behavior (such as being attracted to a fixed plane). In those cases, we successfully used a set with 26 elements:

$V_1 = 2\pi\{\langle i,j,k \rangle | i,j,k \in \{0,1,2\}\} \setminus \{\langle 0,0,0 \rangle\}$. Some of the space groups also required a hexagonal lattice. In that case, we post-multiplied by an extension of the above matrix that added trailing zeros and a row 0 0 1.

We required our functions to pass certain tests before we would consider creating images of their attractors. We checked the first few iterates of our functions to avoid unboundedness, periodicity and collinearity of points before performing higher iteration. For the planar groups we also required the first Ljapunov exponent to be between 0.05 and 0.6. For the space groups, we demanded the first Ljapunov exponent to be between 0.01 and 0.6 and the sum of the first and the second to be negative. This requirement on

the first two Ljapunov exponents is indicative of chaos and a fairly low Ljapunov dimension which was intended to make rendering in three dimensions plausible.

These functions were iterated in J. For the planar groups the resulting attractor was rendered using J. For the space groups the J results were formatted and piped to the raytracing program POV-Ray [24] which may be obtained at the web address <http://www.povray.org>. The Appendix contains the J expressions, including the parameters, used to generate our function with the symmetry of space group 92.

We wanted to make sure our images had a feel of connectedness and nontriviality, thus we checked that there were no empty rows, columns, or planes after resolving the points on the attractor into discrete positions in space. Further, we wanted to avoid the appearance of a repeating isolated motif under the symmetry operations. This led us to the following notion.

Definition. An attractor is **cell-connected** with respect to a lattice if we can get from any cell of the lattice to any other cell by traveling along some part of the attractor.

This property would seem difficult to prove analytically for any nontrivial attractor; however we tried visually to require it. After checking our images for cell-connectedness, we ran prospective images at higher iteration. Even with these tests we note that on very careful inspection of some of our animations, the attractor does not appear to be cell-connected. In order to observe the structure of our attractors in three dimensions, we found it necessary to remove points visited with a frequency below a threshold that ranged from 0 to 20. Thus an attractor may be cell-connected while the skeleton that we rendered might not be cell-connected.

4. Our Planar Examples

Before exploring the examples in \mathcal{R}^3 in Section 5, we will highlight attractors generated by functions in \mathcal{R}^2 produced with the general constructions from Section 2. This allows us to illustrate attractors with translational symmetry, point group symmetry, point group symmetry compatible with the lattice, and general crystallographic symmetry. Observing these examples will be helpful because the symmetries are more evident at a glance in two dimensions than they are in three dimensions.

Figure 1 is an example of an image generated using a function of the form found in Proposition 1, where the function is equivariant with respect to the translational symmetries on the standard lattice L . Thus, this group has p1 symmetry as designated in [16]. The colors are based on the number of times the pixels are hit. Points hit the least number of times by the function are colored red while those hit most often are shaded magenta. The color variation between red and magenta uses a logarithmic bias hence the appearance of more red than magenta. The same scheme was used for the palette in all our images.

Figure 2 was created by summing a function over the symmetries of D_7 as in Proposition 2. The initial function before summing over these symmetries has the form of a bump function in two variables as in [12]. The i -th output of our bump function B is

given by $B(\vec{x})_i = \sum_{0 \leq j \leq 2} a_{ij} e^{-2(x_i - j/2)^2}$ where $0 \leq i \leq 1$ and $a_{ij} \in \mathfrak{R}$. Note that the form of the

function B that we happened to use has no bearing on the symmetry.

Figure 3 is an image showing the attractor of a function of the type in Corollary 3. In other words, we first create a function equivariant to the translational symmetries (as in Proposition 1) and then we sum over the symmetries of D_3 . Note that D_3 preserves the hexagonal lattice L ; hence, our function is equivariant with respect to both the lattice and the symmetries of $D_3 \bmod L$, and we do not need the auxiliary function from Theorem 6 or Porism 7. This attractor has p3m1 symmetry.

Our last planar image in the plane has p2gg symmetry. It is created from a function of the form defined in Porism 7. The generators used to compute the group are

$$\gamma_1 \begin{pmatrix} x \\ y \end{pmatrix} = \begin{pmatrix} -x \\ -y \end{pmatrix} \text{ and } \gamma_2 \begin{pmatrix} x \\ y \end{pmatrix} = \begin{pmatrix} \frac{1}{2} - x \\ \frac{1}{2} + y \end{pmatrix}. \text{ In Figure 4 we can see glide reflections running}$$

both horizontally and vertically.

5. Our Three Dimensional Examples

Our first three dimensional example is an attractor with relatively simple symmetry, that of space group 19. The position group contains only four elements. From [16], we can see that there should be 2-fold screw rotations in the three axial directions.

Screw rotations are a rotation of $\frac{2\pi}{n}$ about a given axis, followed by a translation along the axis. Moreover, if we project onto any of the coordinate planes, we should see the planar crystallographic symmetry group p2gg. Figure 5 provides an overview of a 3 by 3 by 3 arrangement of fundamental cells, in which we can see some of the screw rotations. Figure 6 provides a closer look at the symmetry within the attractor. Notice a 2-fold screw rotation along one of the axes; one can imagine further tipping the attractor to see the p2gg symmetry. Some features of these three dimensional attractors are easier to see via animations where perspective varies. Such an animation may be accessed via the webpage <http://www.lafayette.edu/~reiterc/cacs>. The parameters used for constructing this attractor are also available in a script at that site.

The second attractor we examine exhibits the symmetries of space group 53. Figure 7 provides us with a greater sense of the lattice structure than the previous example. Notice the gaps on both the top and bottom of the attractor. The reason for these gaps is that the attractor has slight deformations away from the layer and hence was truncated so the top and bottom level together form a complete level. A similar remark applies to the sides. While the attractor has a somewhat coarse appearance, one gets a full sense of the attractor's symmetries from this view. From [16], we see that there should be examples of 2-fold screw rotations in one direction and half turns in another direction. The half-turn symmetry and glide reflections of p2gm are apparent in the roughly horizontal levels which is expected. On the completed left/right planes we see the symmetry group c2mm. While on the front/back planes, we can find examples of the half-turns and perpendicular mirrors of the planar symmetry group p2mm.

The next chaotic attractor provides an example of space group 92 symmetry. Figure 8 gives us an overview of the attractor. Figure 9 lets us see the 4-fold screw rotations along one axis and the 2-fold screw rotations along another axis as well as a near p4gm projection, all of which are expected from [16]. Figure 10 gives us intriguing glimpses of glide reflections and mirrors. Slide 175 in the animation for this group displays the pmg symmetry rather nicely. Figure 11 gives us some sense of the many screw rotations involved in the symmetry of space group 92.

Our next example, space group 164, involves a hexagonal lattice which is apparent in Figure 12. This space group contains p6mm symmetry when projected along one axis. You can see the three fold rotations and six fold rotations of p6mm symmetry in that figure. In Figure 13, one can see the two-fold rotations that are expected.

Our last example, space group 227, is the most complicated of our examples. The position group contains 192 elements making computations of the form in Porism 7 rather substantial. Indeed, finding a visually interesting attractor for this group was most challenging because experiments ran slowly: the position group was large and the extended set V_1 was required. Even though the rendering of the attractor is coarse, Figure 14 gives us a feel of how complicated the attractor is. Here we can see some 4-fold screw axes, some half turns, and some mirrors.

The animations available via <http://www.lafayette.edu/~reiterc/cacs> include chaotic attractors with the symmetry of space groups 2, 4, 12, 14, 15, 18, 19, 35, 43, 53, 62, 64, 73, 92, 135, 141, 162, 164, 166, 194, 199, 205, 225, and 227.

6. Conclusion

We have seen that we can create functions with the symmetry of the crystallographic groups by taking a lattice preserving function, summing over the conjugates of the position group for the crystallographic group, and adding the identity function or an auxiliary function. By choosing the parameters of the lattice preserving function carefully, we obtain a chaotic attractor. This provides a uniform method for creating chaotic attractors with planar crystallographic symmetry. The same method gives us attractors with space group symmetry and we render these in three dimensions for striking examples of objects with crystallographic symmetry in space. The technique can also be used to create functions with crystallographic symmetry in higher dimensions.

Acknowledgments —This work was supported by NSF grant DMS-9805507 and Lafayette College. Joachim Neubüser's reply to an e-mail query was very helpful and much appreciated.

References

1. Weyl, H., *Symmetry*, Princeton University, Princeton, NJ, 1952.
2. Gleick, J., *Chaos: Making a New Science*, Penguin Books, New York, 1987.
3. Lorenz, E., Deterministic nonperiodic flow. *Journal of Atmosphere Science*, 1963, **20**, 13-141.
4. Stewart, I. and Golubitsky, M., *Fearful Symmetry: Is God a Geometer?*, Blackwell, Oxford, 1992.

5. Bentley, W. A. and Humphreys, W. J., *Snow Crystals*, Dover Publications, New York, 1962.
6. Zaslavsky, G. M., Sagdeev, R. Z., Usikov, D. A., *Weak Chaos and Quasi-regular Patterns*, Cambridge University Press, Cambridge, 1991.
7. Brisson, G., Gartz, K., McCune, B., O'Brien, K. and Reiter, C., Symmetric attractors in three-dimensional space. *Chaos, Solitons & Fractals*, 1996, **7**, 1033-1051.
8. Carter, N., Eagles, R., Grimes, S., Hahn, A. and Reiter, C., Chaotic attractors with discrete planar symmetries. *Chaos, Solitons & Fractals*, 1998, **9**, 2031-2054.
9. Dumont, J., Heiss, F., Jones, K., Reiter, C. and Vislocky, L., Chaotic attractors and evolving planar symmetry. *Computers & Graphics*, 1999, **23**, 613-619.
10. Dumont, J. and Reiter, C., Chaotic attractors near forbidden symmetry. *Chaos, Solitons & Fractals*, to appear.
11. Field, M. and Golubitsky, M., *Symmetry in Chaos*, Oxford University Press, New York, 1992.
12. Jones, K. and Reiter, C., Chaotic attractors with cyclic symmetry revisited. *Computers & Graphics*, to appear.
13. Reiter, C., Attractors with the symmetry of the n -cube. *Experimental Mathematics*, 1996, **5**, 327-336.
14. Reiter, C., Chaotic attractors with the symmetry of the tetrahedron. *Computers & Graphics*, 1997, **21**, 841-848.
15. Reiter, C., Chaotic attractors with the symmetry of the dodecahedron. *The Visual Computer*, 1999, **15**, 211-215.
16. Hahn, T., *International Tables for Crystallography*, Kluwar Academic Publishers, Boston, ed. 1996.
17. Iversen, B., *Lectures on Crystallographic Groups, Lecture Note Series no. 60*, Aarhus: Aarhus Universitet Matematisk Institut, 1995.
18. Grunbaum, B. and Shepard, G., *Tilings and Patterns*, W. H. Freeman, New York, 1987.
19. Hahn, T., *International Tables for Crystallography: Brief Teaching Edition, Volume A*, Kluwar Academic Publishers, Boston, ed. 1996.
20. Barany, E., Dellnitz, M. and Golubitsky, M., Detecting the symmetry of attractors. *Physica D*, 1993, **61**, 66-87.
21. Brown, G., Bülow, R., Neubüser, J., Wondratschek, H. and Zassenhaus, H., *Crystallographic Groups of Four-Dimensional Space*, John Wiley & Sons, New York, 1978.
22. Ascher, E. and Janner, A., Algebraic Aspects of Crystallography II Non-primitive Translations in Space Groups. *Communications in Mathematical Physics*, 1968, **11**, 138-167.
23. Speiser, A., *Die Theorie der Gruppen von enlicher Ordnung, mit Anwendungen auf algebraische Zahlen und Gleichungen sowie auf die Krystallographie*, ed 4, Birkhäuser, Basel, 1956.
24. Wegner, T., *Image Lab*, Waite Group Press, Corte Madera, CA, 1992.
25. Hui, R. and Iverson, K., *J Dictionary*, Iverson Software Inc., Toronto, 1998.

Appendix A

Our functions were implemented in J [25] which may be obtained at <http://www.jsoftware.com>. The following J expressions allow one to duplicate the construction of one function. This is the function whose attractor is displayed in Figures 8-11. A script which includes the expressions, including all parameter values for all the functions used to create the 24 animations, can be found at <http://www.lafayette.edu/~reiterc/cacs>.

```

sin=:1&o.
cos=:2&o.
x=:+/. *
]V=:2p1*#:4 2 1 7
6.28319      0      0
      0 6.28319      0
      0      0 6.28319
6.28319 6.28319 6.28319
proj=: 1 : '({:{"1 +./m.~:0)&*'
prop1=:1 : '1&|@:(+/^:2@:(m."_*(sin,:cos)@:(V&x))) f.'
prop3a=:2 : 'n. proj 1&|@:+ +/@:({:"1)@((%.n.)&(x"2
1)@:(, &1@u.@}:"1@ (n.&x@ (, &1))) f.'
par
_0.00413499 0.00327672 _0.0281041
_0.0452955 0.0178865 0.0179296
0.0434693 _0.0116498 0.00194164
0.0330965 _0.0465428 _0.0446538

0.00297002 0.0171149 _0.0492302
_0.0116584 _0.0433158 _0.0082514
0.0186773 0.00889766 0.0430436
0.0346167 0.00269288 _0.0408035

pos=: \:~@~.@(* >&1e_14@:|)@ (, , /@:((((<: (*. -.@|:)@:=
      ]"0/~@i.)@{:@$|])@(+/. *.))"2/~)) ^:_
h001=:1 0 0 0, 0 1 0 0, 0 0 1 0.5,:0 0 0 1
i110=:_1 0 0 0,0 _1 0 0 ,0 0 1 0,:0 0 0 1
gen1=:h001 x i110
gen2=:_1 0 0 0.5,0 1 0 0.5,0 0 _1 0.25,:0 0 0 1
gen3=:0 _1 0 0.5,1 0 0 0.5,0 0 1 0.25,:0 0 0 1
$p092=: pos gens=:gen1,gen2,:gen3
8 4 4

```

Sine function
Cosine function
Matrix multiplication
Elements of the dual basis

Array of parameters

Group closure

$2 \ 4\$<"2 \ G=:p092$

Position group elements

1 0 0 0.5	1 0 0 0	0 1 0 0.5	0 1 0 0
0 _1 0 0.5	0 1 0 0	_1 0 0 0.5	1 0 0 0
0 0 _1 0.75	0 0 1 0	0 0 1 0.75	0 0 _1 0
0 0 0 1	0 0 0 1	0 0 0 1	0 0 0 1
0 _1 0 0.5	0 _1 0 0	_1 0 0 0.5	_1 0 0 0
1 0 0 0.5	_1 0 0 0	0 1 0 0.5	0 _1 0 0
0 0 1 0.25	0 0 _1 0.5	0 0 _1 0.25	0 0 1 0.5
0 0 0 1	0 0 0 1	0 0 0 1	0 0 0 1

 $F092=: \text{par prop1 prop3a } G$

The function definition

 $F092^:(i.5) \ 0.1 \ 0.2 \ 0.3$

The first few iterates

```

0.1      0.2      0.3
0.514702 0.734087 0.877241
0.670501 0.286339 0.708132
0.0564265 0.364323 0.175236
0.86939 0.395658 0.0350441

```

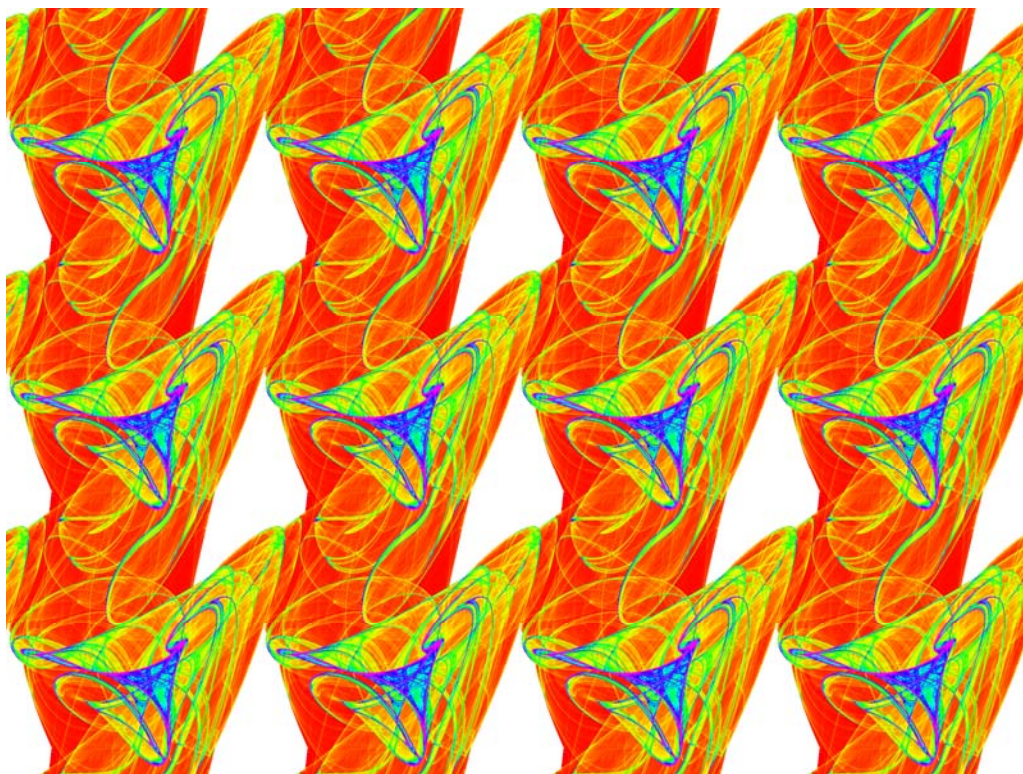


Figure 1. A chaotic attractor with p1 planar crystallographic symmetry.

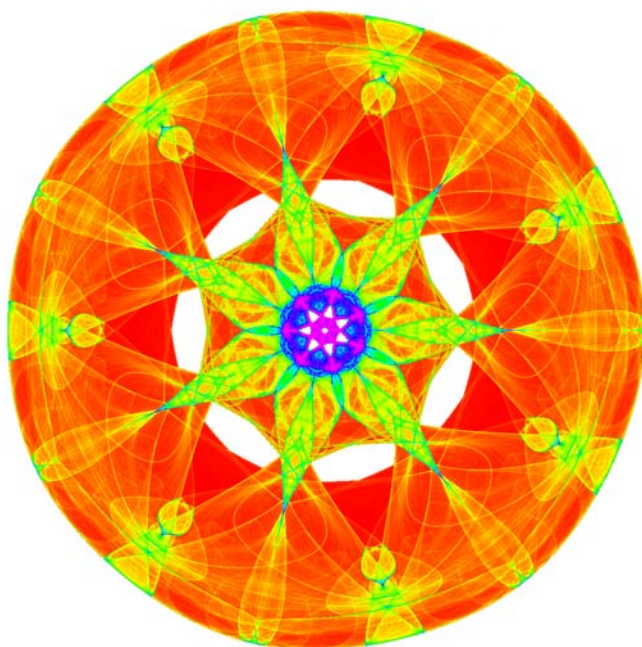


Figure 2. A chaotic attractor with dihedral D_7 symmetry.

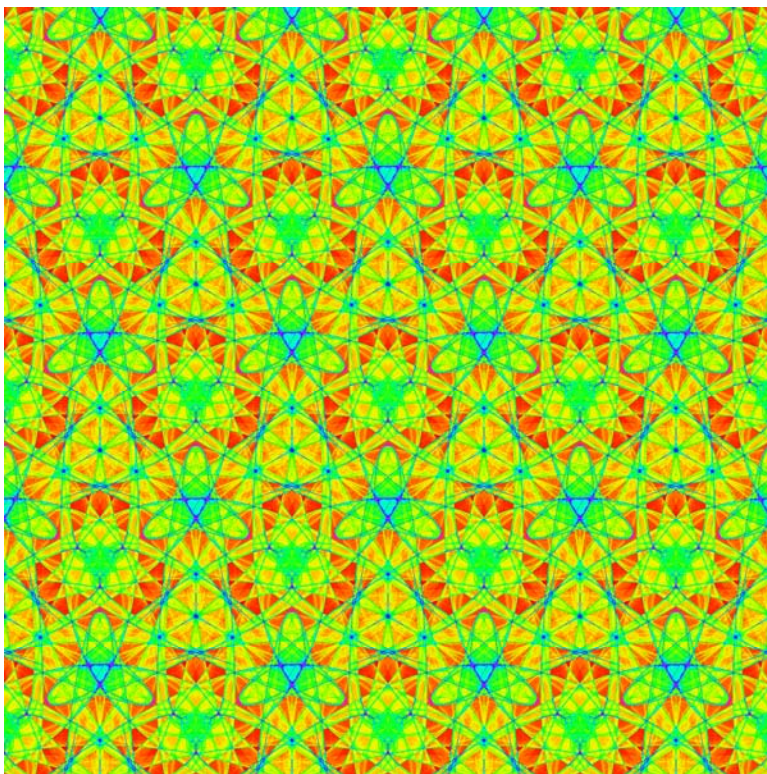


Figure 3. A chaotic attractor with $p3m1$ planar crystallographic symmetry.

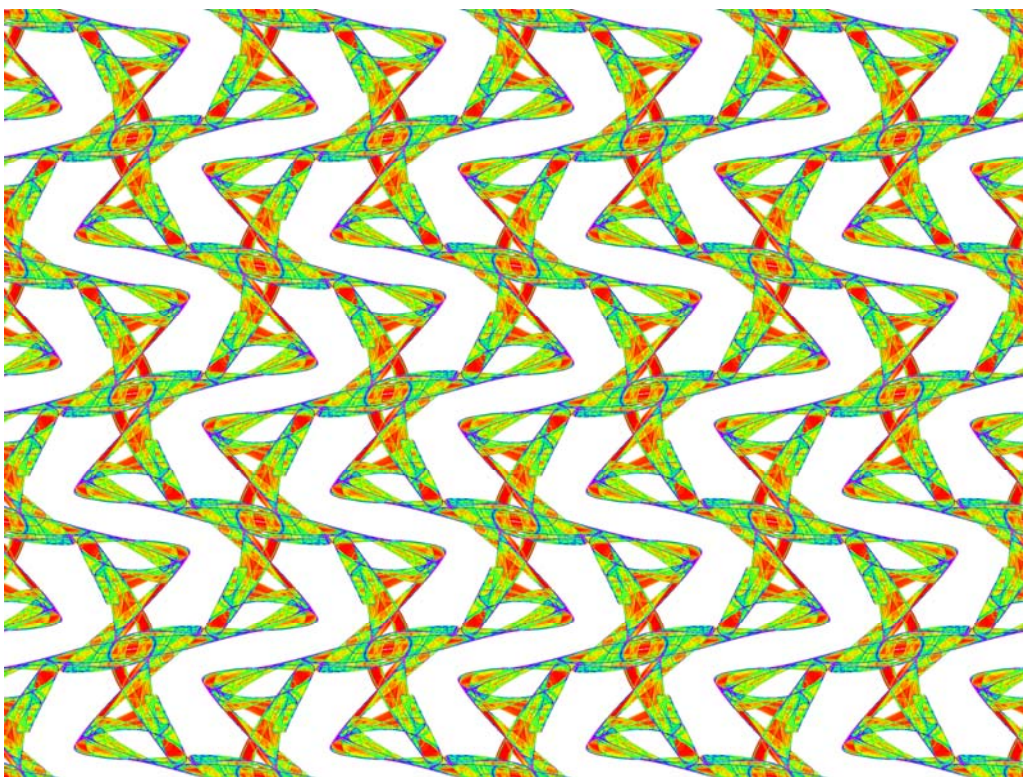


Figure 4. A chaotic attractor with $p2gg$ planar crystallographic symmetry.

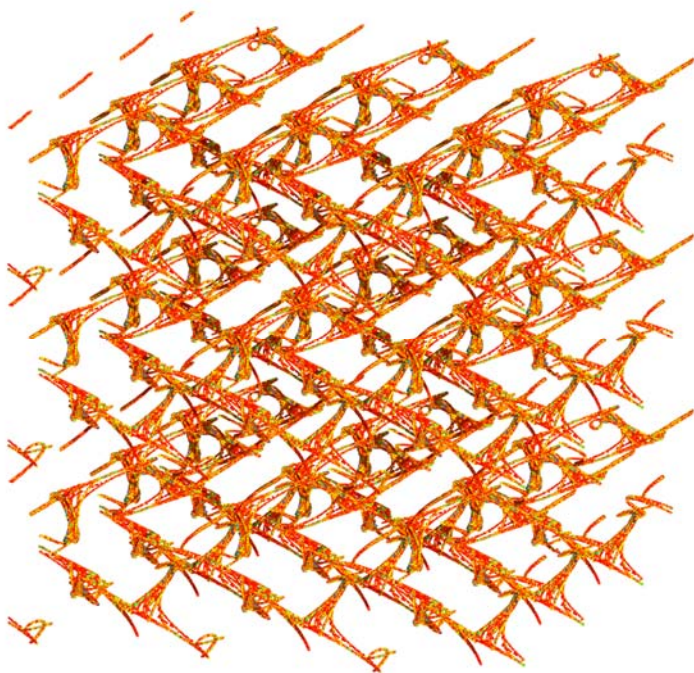


Figure 5. An overview of a chaotic attractor with space group 19 symmetry.

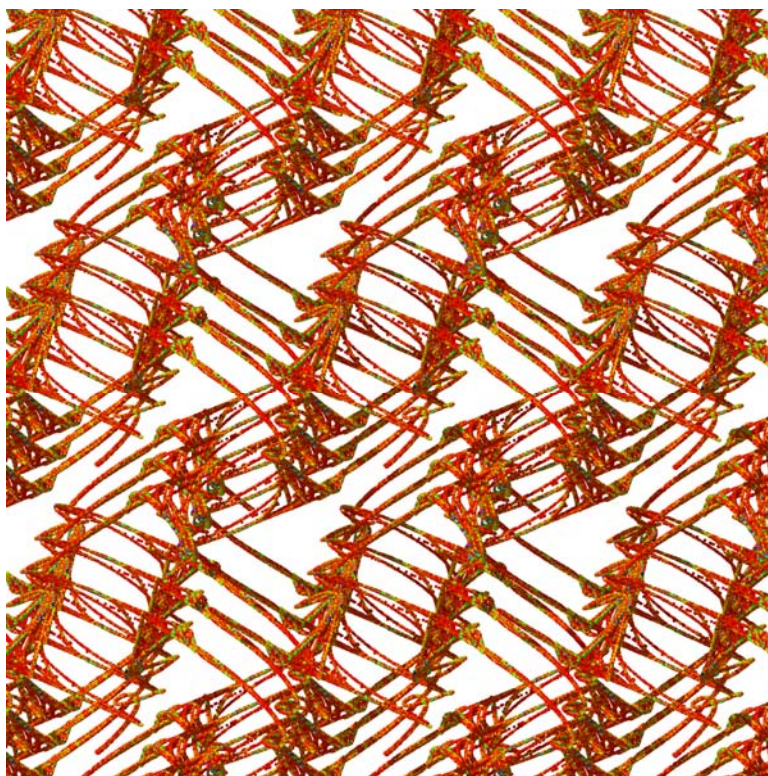


Figure 6. A chaotic attractor with space group 19 symmetry with projection near p2gg symmetry.

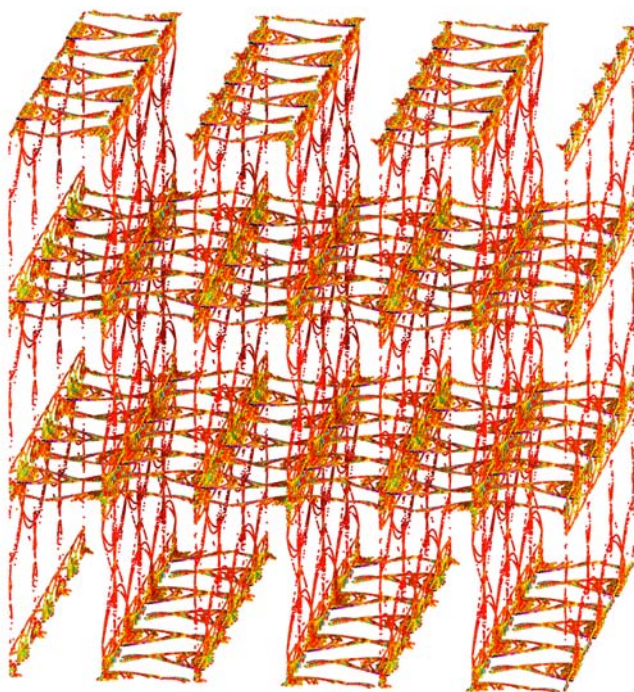


Figure 7. An overview of a chaotic attractor with space group 53 symmetry.

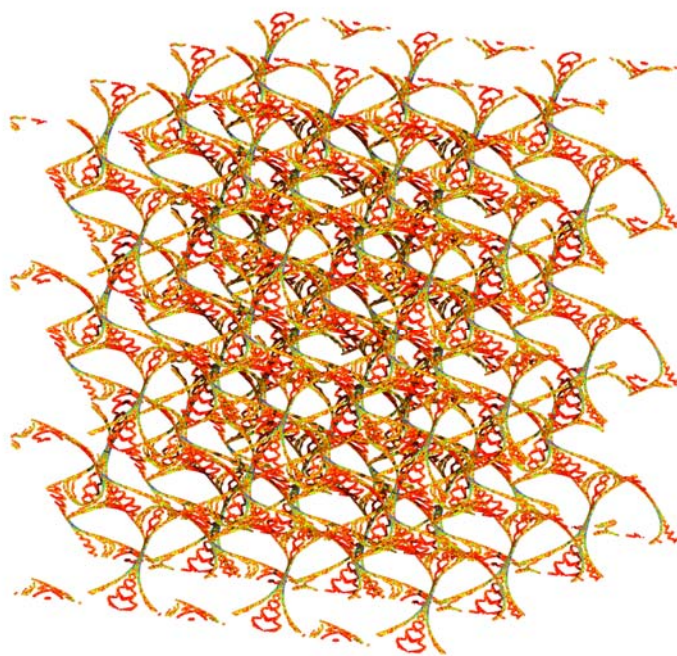


Figure 8. An overview of a chaotic attractor with space group 92 symmetry

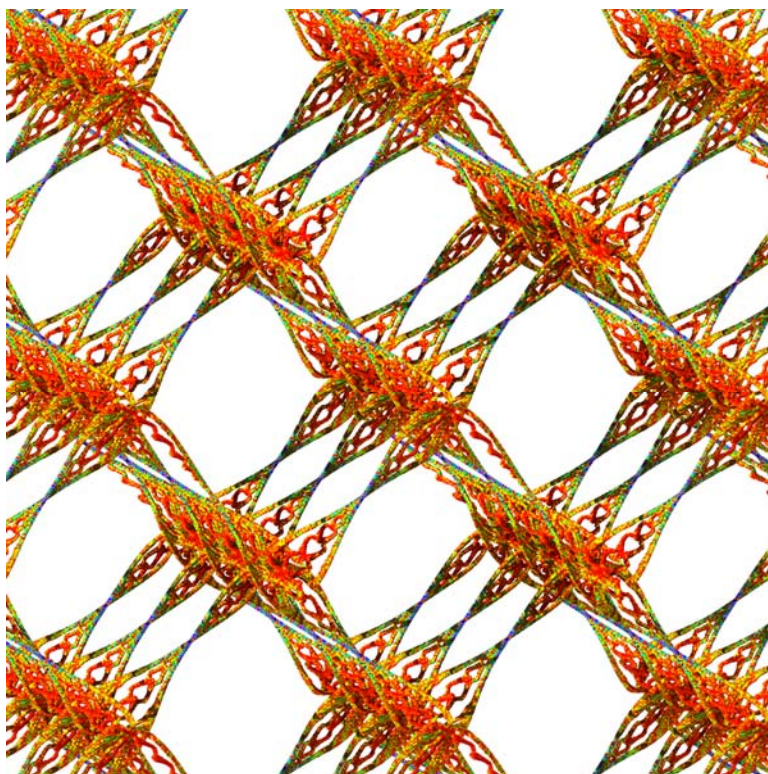


Figure 9. A chaotic attractor with space group 92 symmetry and visible 4-fold screw rotations.

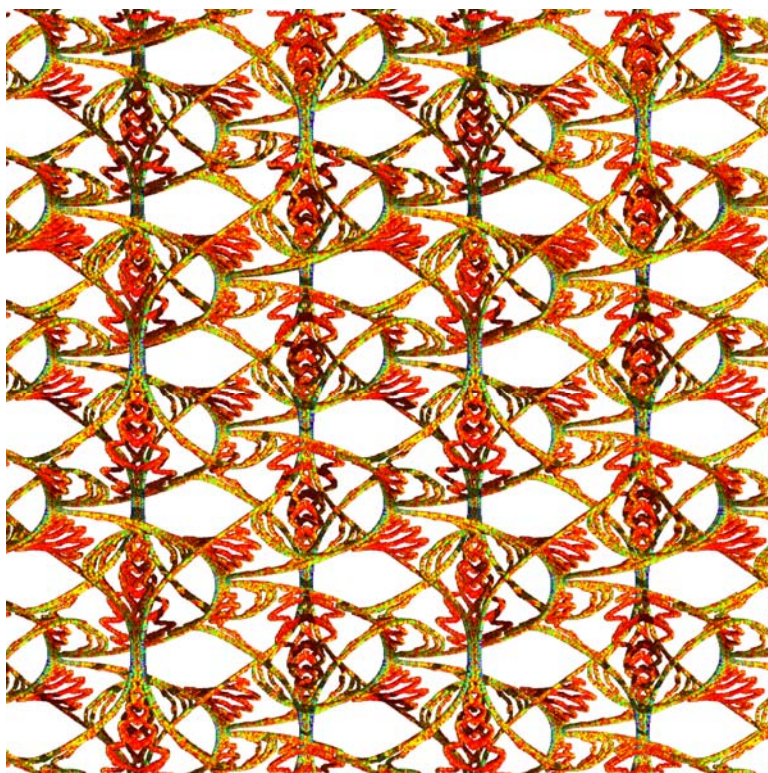


Figure 10. A chaotic attractor with space group 92 symmetry and suggestions of mirrors and glides.

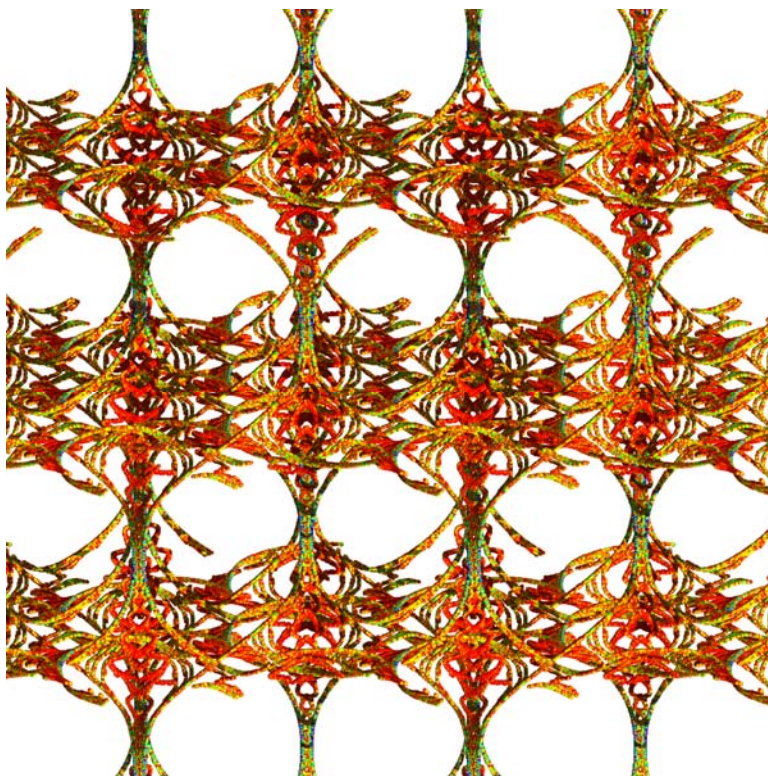


Figure 11. A chaotic attractor with space group 92 symmetry and visible screw rotations.

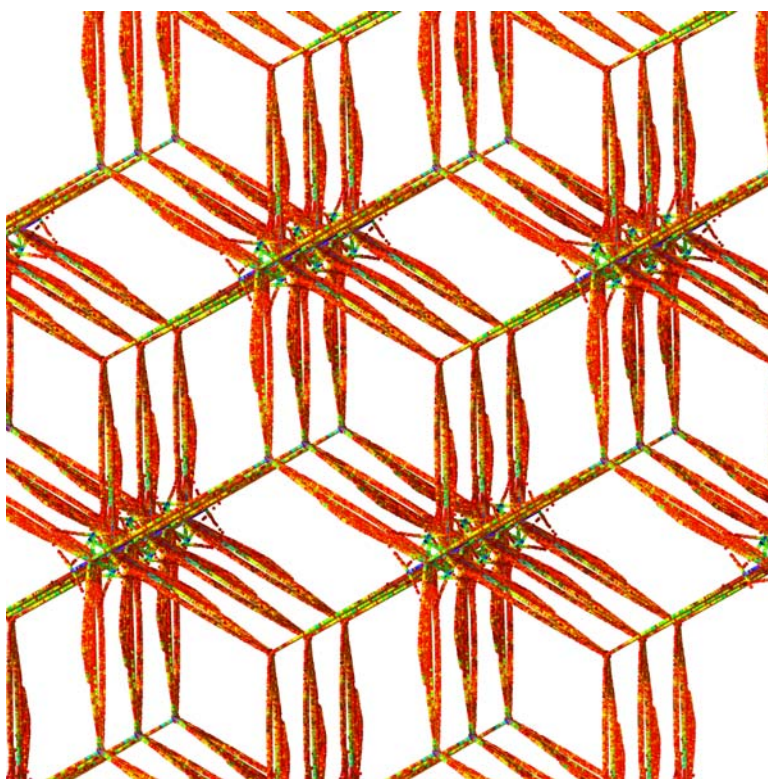


Figure 12. A chaotic attractor with space group 164 symmetry and visible third and sixth turns.

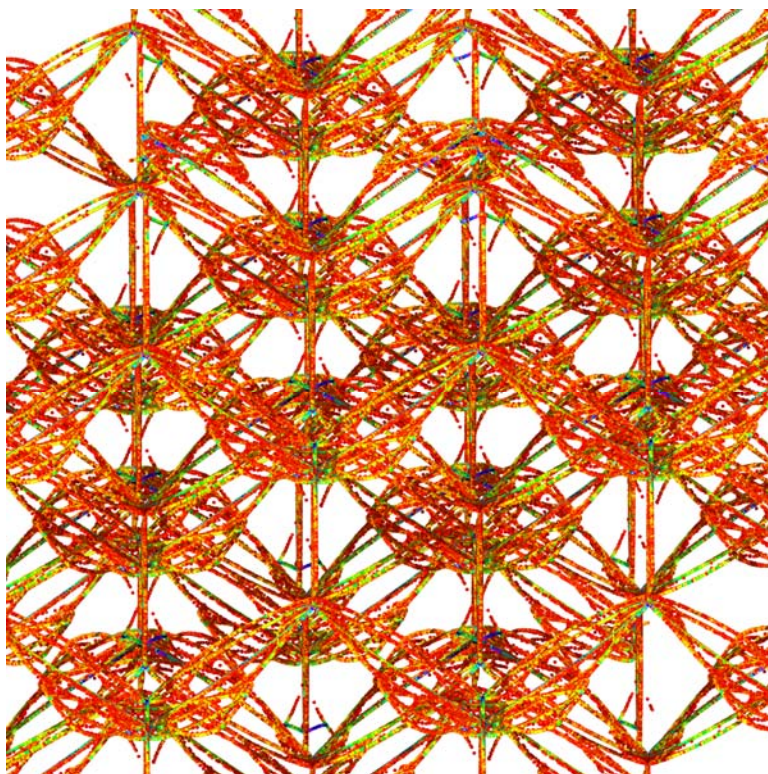


Fig. 13. A chaotic attractor with space group 164 symmetry and 2-fold rotations.

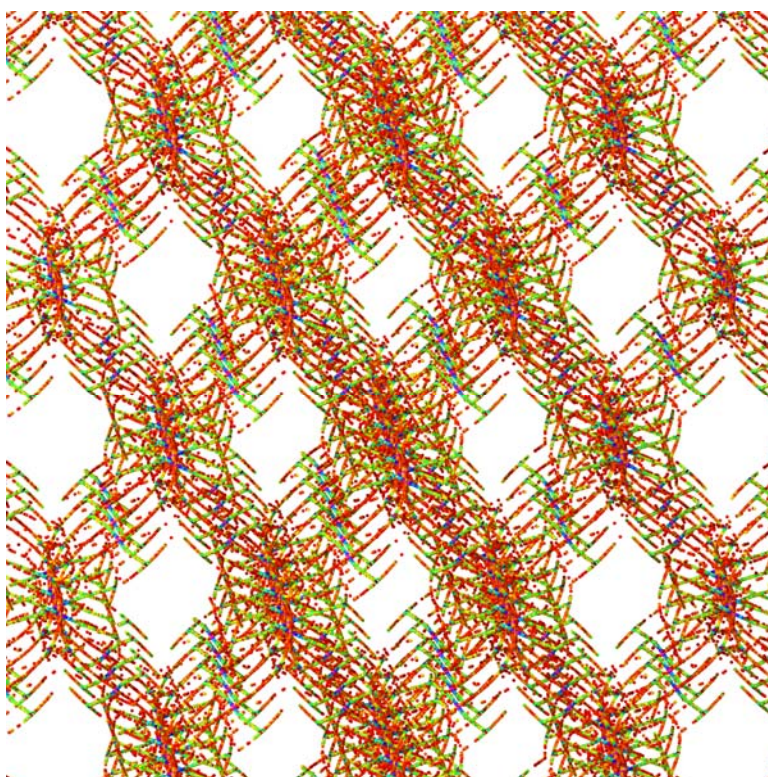


Fig. 14. A chaotic attractor with space group 227 symmetry